Signal Processing 89 (2009) 1715–1722

Contents lists available at ScienceDirect

Signal Processing

journal homepage: www.elsevier.com/locate/sigpro

Efficient underwater two-dimensional coherent source localization with linear vector-hydrophone array

Jin He *, Zhong Liu

Department of Electronic Engineering, Nanjing University of Science and Technology, Nanjing, Jiangsu 210094, China

ARTICLE INFO

Article history:
Received 15 September 2008
Received in revised form
28 February 2009
Accepted 9 March 2009
Available online 24 March 2009

Keywords:
Array signal processing
Direction finding
Source localization
Multipath
Coherent signal
Vector hydrophone
Propagator method

ABSTRACT

This paper proposes a new computationally simple 2D direction finding algorithm for underwater acoustic coherent signals using a uniformly linear array of vector hydrophones. We decorrelate the source coherency by subarray averaging, and apply the *propagator method* to estimate automatically paired direction cosines embedded in the acoustical particle-velocity components of the vector hydrophone. Therefore, the presented algorithm requires neither the eigen-decomposition into signal/noise subspaces nor the 2D iteratively searching. In addition, because the vector-hydrophone array manifold contains no sensor location information, this new algorithm can offer high azimuth–elevation estimation accuracy by setting vector hydrophones to space much farther apart than a half-wavelength. The presented algorithm can be regarded as an improvement of SUMWE algorithm [19] via replacing the pressure hydrophones there by vector hydrophones. Monte-Carlo simulations are presented to verify the efficacy of the proposed algorithm.

1. Introduction

Source localization using an array of vector hydrophones has played a fundamental role in underwater signal processing. A vector hydrophone is three or four components in composition, consisting of two or three velocity hydrophones plus a pressure hydrophone, collocated in space. During the last decade, many subspace-based techniques, such as MUSIC [1] and ESPRIT [2], have been combined with vector hydrophones to estimate 2D directions of underwater narrowband signals. (see e.g., [3–10].) Typically, these methods use the eigen-decomposition (or singular value decomposition) to decompose the column space of the data correlation matrix into a signal subspace and a noise subspace, and the signal directions are extracted based on the particle-velocity diversity in addition with the spatial diversity. The additional information made by the velocity hydrophones offers many advantages, e.g., arbitrary array geometry [4], sparse array aperture extension [5], to improve angle estimation accuracy over the conventional pressure hydrophone-based methods. Unfortunately, this additional information also increases the data dimensions to be eigen-decomposed, and the eigen-decomposition process is computationally intensive and time-consuming. Consequently, these subspace-based methods are unsuitable for applications where the number of sensors is large and/or the directions of impinging signals should be tracked promptly.[1]

Furthermore, all of the above mentioned methods assume incoherent signals, i.e., that the signal covariance

* Corresponding author.
E-mail address: andrie1111@hotmail.com (J. He).

[1] We stress that there exist many computationally efficient eigen-decomposition methods, such as adaptive eigen-decomposition with rank one perturbations [11], computing only a few eigenvectors [12], and recursively updating the eigenvectors [13]. However, in this paper, we consider computationally efficient method, which avoids the need for computation of eigen-decomposition.

0165-1684/$ - see front matter © 2009 Elsevier B.V. All rights reserved.
doi:10.1016/j.sigpro.2009.03.008

matrix has full rank. This assumption is often violated in scenarios where multipath exists. Coherent signals could reduce the rank of signal covariance matrix below the number of incident signals, and hence, degrade critically the algorithmic performance. To deal with the coherent signals using hydrophone array, [14] proposes to restore the rank of signal subspace by smoothing across the particle-velocity-component's data correlation matrices. This particle-velocity smoothing technique does not reduce the array's spatial aperture, however, it requires a planar array geometry and/or 2D iteratively searching to estimate 2D directions of incoming signals. Moreover, the particle-velocity smoothing needs the inter-hydrophone spacing within a half-wavelength to guarantee unique and unambiguous angle estimates.

Therefore, the contribution of this work is to propose a new computationally efficient direction finding algorithm for coherent signals using a uniformly linear array of vector hydrophones. Firstly, we decorrelate the signal coherency via subarray averaging. Then, the so-called propagator method[2] is applied to estimate the vector-hydrophone array manifolds. Finally, closed-form automatically paired azimuth–elevation angle estimates are derived. The proposed algorithm does not need to compute all correlations of array data, requires no eigendecomposition into signal or noise subspaces, and involves no 2D iteratively searching. In addition, because the vector-hydrophone array manifold contains no time-delay phase factor, the proposed algorithm may not suffer direction cyclical ambiguity when the inter-hydrophone spacing extends beyond a half-wavelength. The inherent structure of hydrophone sensor also allows the array aperture extension to offer enhanced angle estimation precision. Moreover, the presented algorithm can be considered as an improvement of SUMWE algorithm [19] via replacing the pressure hydrophone there by vector hydrophones. Unlike SUMWE algorithm, the proposed algorithm extract the angles of the incoming signals from the particle-velocity information embedded in a vector hydrophone, but not from the spatial phase information between two adjacent sensors. Thus, as mentioned above, the proposed algorithm exploits the benefits inherent in the additional measurements made by the vector hydrophones to achieve 2D angle estimation with a linear array geometry.

The rest of this paper is organized as follows. Section 2 formulates the mathematical data model of the present problem. Section 3 develops the proposed algorithm. Section 4 presents the simulation results to verify the efficacy of the proposed algorithm. Section 5 concludes the paper.

Throughout the paper, scalar quantities are denoted by regular lowercase letters. Lowercase bold type faces are used for vectors and regular uppercase letters for matrices. Superscripts T, H, $*$, and $\dagger$ represent the transpose, conjugate transpose, complex conjugate and pseudo inverse, respectively. $\otimes$ symbolizes the Kronecker-product operator. $\mathbf{0}_{m,n}$ and $\mathbf{I}_m$ denote the $m\times n$ zero matrix and $m\times m$ identity matrix, respectively.

[2] The 'propagator' was first defined in [15]. The propagator method offers estimation accuracy comparable to that of its subspace-based counterparts, but requires a much reduced computational complexity. There exist many propagator-based direction finding algorithms using the pressure-hydrophone array. We refer to [16–20] for reference.

2. Mathematical data model

Consider K narrowband planer wave source signals, parameterized by $\{\theta_1,\phi_1\},\{\theta_2,\phi_2\},\ldots,\{\theta_K,\phi_K\}$, impinge upon a ULA of L vector hydrophones. Each vector hydrophone used here has three components, i.e., two velocity hydrophones and a pressure hydrophone, co-located in space. The vector hydrophone's 3×1 manifold with regard to the kth signal is defined by [4]

$$\mathbf{c}(\theta_k,\phi_k)\overset{\text{def}}{=}\begin{bmatrix}c_1\\c_2\\c_3\end{bmatrix}\overset{\text{def}}{=}\begin{bmatrix}1\\u_k\\v_k\end{bmatrix}\overset{\text{def}}{=}\begin{bmatrix}1\\u(\theta_k,\phi_k)\\v(\theta_k,\phi_k)\end{bmatrix}=\begin{bmatrix}1\\\sin\theta_k\cos\phi_k\\\sin\theta_k\sin\phi_k\end{bmatrix} \tag{1}$$

where $0\leqslant\theta_k<\pi$ denotes the kth signal's elevation angle, and $0\leqslant\phi_k<2\pi$ represents the kth signal's azimuth angle. u_k and v_k signify the direction cosines along the x-axis and y-axis, respectively. The first component of (1), corresponding to the pressure hydrophone, and the remaining two components of (1) correspond to the velocity hydrophone aligned along x-axis and y-axis, respectively. Note that, the vector-hydrophone array manifold contains no time-delay phase factor. That is, the vector-hydrophone array manifold is independent of the impinging signals' frequency spectra [8]. This fact is pivotal to improve the estimation accuracy by array aperture extension beyond spatial Nyquist sampling theorem.

The inter-hydrophone spatial phase factor for the kth incident signal and the ℓth vector hydrophone is [4]

$$q_\ell(\theta_k,\phi_k)=e^{j2\pi x_\ell u_k/\lambda}e^{j2\pi y_\ell v_k/\lambda}=e^{j2\pi(x_\ell u_k+y_\ell v_k)/\lambda} \tag{2}$$

where (x_ℓ,y_ℓ) is the location of the ℓth vector hydrophone. Denoting the components of spacing between adjacent hydrophones as (Δ_x,Δ_y), we have

$$x_\ell=x_1+(\ell-1)\Delta_x \tag{3}$$

$$y_\ell=y_1+(\ell-1)\Delta_y \tag{4}$$

Then, the $3L\times 1$ array manifold of the entire vector-hydrophone array is

$$\mathbf{a}(\theta_k,\phi_k)=\begin{bmatrix}\mathbf{a}_1(\theta_k,\phi_k)\\\vdots\\\mathbf{a}_L(\theta_k,\phi_k)\end{bmatrix}=\begin{bmatrix}q_1(\theta_k,\phi_k)\\\vdots\\q_L(\theta_k,\phi_k)\end{bmatrix}\otimes\mathbf{c}(\theta_k,\phi_k) \tag{5}$$

It follows from (5) that

$$\mathbf{a}_\ell(\theta_k,\phi_k)=q_\ell(\theta_k,\phi_k)\mathbf{c}(\theta_k,\phi_k) \tag{6}$$

With a total of K signals, the entire $3L\times 1$ output vector measured by the vector-hydrophone array at time t has the complex envelope represented as

$$\begin{aligned}\mathbf{z}(t)&=\sum_{k=1}^{K}\mathbf{a}(\theta_k,\phi_k)s_k(t)+\mathbf{n}(t)=\mathbf{A}\mathbf{s}(t)+\mathbf{n}(t)\\&=\mathbf{A}\boldsymbol{\beta}s_1(t)+\mathbf{n}(t)\end{aligned} \tag{7}$$

where $\mathbf{A} \stackrel{\text{def}}{=} [\mathbf{a}(\theta_1,\phi_1),\ldots,\mathbf{a}(\theta_K,\phi_K)]$; $\mathbf{n}(t) \stackrel{\text{def}}{=} [n_1(t),\ldots,n_{3L}(t)]^T$ refers to the $3L\times 1$ additive zero-mean complex noise and is independent to all signals. The matrix $\mathbf{A}$ has the structure

$$\mathbf{A} = [\mathbf{A}_0^T, (\mathbf{A}_0\mathbf{D})^T, (\mathbf{A}_0\mathbf{D}^2)^T, \ldots, (\mathbf{A}_0\mathbf{D}^{L-1})^T]^T \tag{8}$$

with $\mathbf{A}_0$ being the first three rows of $\mathbf{A}$, and $\mathbf{D} \stackrel{\text{def}}{=} \text{diag}\{e^{j(2\pi/\lambda)(\Delta_x u_1+\Delta_y v_1)},\ldots,\ e^{j(2\pi/\lambda)(\Delta_x u_K+\Delta_y v_K)}\}$. $\boldsymbol{\beta} \stackrel{\text{def}}{=} [\beta_1,\ldots,\beta_K]^T$, where β_k is the complex attenuation coefficient with $\beta_k \neq 0$ and $\beta_1 = 1$. Throughout the paper, it is assumed that $\mathbf{A}$ is of full rank. The assumption is required for all direction finding algorithms.

Our objective is to determine $\{\theta_k,\phi_k,k=1,\ldots,K\}$ from the N snapshots $\mathbf{z}(t_1),\ldots,\mathbf{z}(t_N)$ taken at the distinct time indices $\{t_n,n=1,\ldots,N\}$.

3. Algorithm development

3.1. Subarray averaging

On the assumption that the incoming signals are coherent, the rank of signal covariance matrix becomes smaller than the number of signals. This subsection will use the subarray averaging technique to handle this rank deficit problem.

Firstly, we divide the full array into M overlapping subarrays with K hydrophones each in the forward and backward manners, where $M = L-K+1$. The mth forward subarray comprises the mth to $(m+K-1)$th vector hydrophone, whereas the mth backward subarray comprises the $(L-m+1)$th to $(M-m+1)$th vector hydrophone. Therefore, the $3K\times 1$ signal vector of the mth forward subarray and the mth backward subarray can be, respectively, expressed as

$$\mathbf{z}_{fm}(t) = \mathbf{A}_1\mathbf{D}^{m-1}\mathbf{s}(t) + \boldsymbol{\omega}_{fm}(t) \tag{9}$$

$$\mathbf{z}_{bm}(t) = \mathbf{A}_1\mathbf{D}^{-(L-m)}\mathbf{s}^*(t) + \boldsymbol{\omega}_{bm}(t) \tag{10}$$

where $\mathbf{D} \stackrel{\text{def}}{=} \text{diag}\{e^{j(2\pi/\lambda)(\Delta_x u_1+\Delta_y v_1)},\ldots,\ e^{j(2\pi/\lambda)(\Delta_x u_K+\Delta_y v_K)}\}$, and $\mathbf{A}_1$ denotes the first $3K$ rows of $\mathbf{A}$.

Then, denoting $z_{\ell,j}(t)$ as the measurement of the ℓth vector hydrophone's jth component, we can calculate the $3K\times 1$ vector between $\mathbf{z}_{fm}(t)$ and $z_{L,j}(t)$

$$\begin{aligned}\mathbf{r}_{fm,j} &= E\{\mathbf{z}_{fm}(t)z_{L,j}^*(t)\}\\ &= E\{\mathbf{A}_1\mathbf{D}^{m-1}\boldsymbol{\beta}s_1(t)s_1^*(t)\boldsymbol{\beta}^H\mathbf{a}_{L,j}^*\} + E\{\boldsymbol{\omega}_{fm}(t)n_{3(L-1)+j}^*(t)\}\\ &= \rho_{L,j}r_s\mathbf{A}_1\mathbf{D}^{m-1}\boldsymbol{\beta},\quad m=1,\ldots,M-1,\ j=1,2,3\end{aligned} \tag{11}$$

where $\rho_{\ell,j} \stackrel{\text{def}}{=} \boldsymbol{\beta}^H\mathbf{a}_{\ell,j}^*$, with $\mathbf{a}_{\ell,j} \stackrel{\text{def}}{=} [q_\ell(\theta_1,\phi_1)\ \ c_j(\theta_1,\phi_1),\ldots,q_\ell(\theta_K,\phi_K)c_j(\theta_K,\phi_K)]^T$. $r_s = E\{s_1(t)s_1^*(t)\}$ is the power of the first signal. This $3K\times 1$ vector can be formed into a $3\times K$ matrix as

$$\mathbf{R}_{fm,j} = [\mathbf{J}_1\mathbf{r}_{fm,j},\mathbf{J}_2\mathbf{r}_{fm,j},\ldots,\mathbf{J}_K\mathbf{r}_{fm,j}] = \rho_{L,j}r_s\mathbf{A}_0\mathbf{D}^{m-1}\mathbf{B}\mathbf{Q}_j^T \tag{12}$$

where $\mathbf{J}_k \stackrel{\text{def}}{=} [\mathbf{0}_{3,3\times(k-1)},\mathbf{I}_3,\mathbf{0}_{3,3\times(K-k)}]$, $\mathbf{B} = \text{diag}[\beta_1,\ldots,\beta_K]$, and the kth column of $\mathbf{Q}_j$ equals $[c_j(\theta_k,\phi_k)q_1(\theta_k,\phi_k),\ldots,c_j(\theta_k,\phi_k)q_K(\theta_k,\phi_k)]^T$. Therefore, concatenating $\mathbf{R}_{fm,j}$ for $m=1,\ldots,M-1$, we can get a correlation matrix

$$\mathbf{R}_{f,j} = [\mathbf{R}_{f1,j}^T,\mathbf{R}_{f2,j}^T,\ldots,\mathbf{R}_{f(M-1),j}^T]^T = \rho_{L,j}r_s\mathbf{A}_M\mathbf{B}\mathbf{Q}_j^T \tag{13}$$

where $\mathbf{A}_M$ contains first $3(M-1)$ rows of $\mathbf{A}$.

In addition, we can compute the following $3K\times 1$ vectors

$$\begin{aligned}\tilde{\mathbf{r}}_{fm,j} &= E\{\mathbf{z}_{fm}(t)z_{1,j}^*(t)\}\\ &= \rho_{1,j}r_s\mathbf{A}_1\mathbf{D}^{m-1}\boldsymbol{\beta},\quad m=2,\ldots,M,\ j=1,2,3\end{aligned} \tag{14}$$

$$\begin{aligned}\mathbf{r}_{bm,j} &= E\{z_{1,j}(t)\mathbf{z}_{bm}(t)\}\\ &= \rho_{1,j}^*r_s\mathbf{A}_1\mathbf{D}^{L-m}\boldsymbol{\beta}^*,\quad m=1,\ldots,M-1,\ j=1,2,3\end{aligned} \tag{15}$$

$$\begin{aligned}\tilde{\mathbf{r}}_{bm,j} &= E\{z_{L,j}(t)\mathbf{z}_{bm}(t)\}\\ &= \rho_{L,j}^*r_s\mathbf{A}_1\mathbf{D}^{L-m}\boldsymbol{\beta}^*,\quad m=2,\ldots,M,\ j=1,2,3\end{aligned} \tag{16}$$

Similar as $\mathbf{R}_{f,j}$ is constructed from $\mathbf{r}_{fm,j}$, we can easily construct $\tilde{\mathbf{R}}_{f,j}$, $\mathbf{R}_{b,j}$ and $\tilde{\mathbf{R}}_{b,j}$ using $\tilde{\mathbf{r}}_{fm,j}$, $\mathbf{r}_{bm,j}$ and $\tilde{\mathbf{r}}_{bm,j}$ as follows:

$$\begin{aligned}\tilde{\mathbf{R}}_{f,j} &= [\tilde{\mathbf{R}}_{f2,j}^T,\tilde{\mathbf{R}}_{f3,j}^T,\ldots,\tilde{\mathbf{R}}_{fM,j}^T]^T\\ &= \rho_{1,j}r_s\mathbf{A}_M\mathbf{B}\mathbf{D}\mathbf{Q}_j^T\end{aligned} \tag{17}$$

$$\begin{aligned}\mathbf{R}_{b,j} &= [\mathbf{R}_{b1,j}^T,\mathbf{R}_{b2,j}^T,\ldots,\mathbf{R}_{b(M-1),j}^T]^T\\ &= \rho_{1,j}^*r_s\mathbf{A}_M\mathbf{B}^*\mathbf{D}^{-(L-1)}\mathbf{Q}_j^T\end{aligned} \tag{18}$$

$$\begin{aligned}\tilde{\mathbf{R}}_{b,j} &= [\tilde{\mathbf{R}}_{b2,j}^T,\tilde{\mathbf{R}}_{b3,j}^T,\ldots,\tilde{\mathbf{R}}_{bM,j}^T]^T\\ &= \rho_{L,j}^*r_s\mathbf{A}_M\mathbf{B}^*\mathbf{D}^{-(L-2)}\mathbf{Q}_j^T\end{aligned} \tag{19}$$

Since $\mathbf{B}$ and $\mathbf{D}$ are diagonal matrices and $\mathbf{Q}_j$ is a $K\times K$ Vandermonde matrix. Using the fact that $\text{rank}(\mathbf{XY}) = \text{rank}(\mathbf{Y})$ if the matrix $\mathbf{X}$ is of full-column rank, it is easy to conclude that $\mathbf{R}_{f,j}$, $\tilde{\mathbf{R}}_{f,j}$, $\mathbf{R}_{b,j}$ and $\tilde{\mathbf{R}}_{b,j}$ are of rank K. Therefore, $\mathbf{R}_{f,j}$, $\tilde{\mathbf{R}}_{f,j}$, $\mathbf{R}_{b,j}$ and $\tilde{\mathbf{R}}_{b,j}$ can be used to estimate the directions of the coherent signals. Finally, we define the following subarray averaged matrix for further processing:

$$\mathbf{R} = [\mathbf{R}_{f,1},\ldots,\mathbf{R}_{f,3},\tilde{\mathbf{R}}_{f,1},\ldots,\tilde{\mathbf{R}}_{f,3},\mathbf{R}_{b,1},\ldots,\mathbf{R}_{b,3},\tilde{\mathbf{R}}_{b,1},\ldots,\tilde{\mathbf{R}}_{b,3}] \tag{20}$$

Note that, the presented method can also be used to the case of partly coherent or incoherent signals. To see this, we assume the first K_1 $(1\leqslant K_1\leqslant K)$ incident signals are coherent and the others are uncorrelated with these signals and with each other, then, after some algebraic manipulations, we can obtain

$$\mathbf{R}_{f,j} = \bar{\rho}_{L,j}r_{s_1}\mathbf{A}_M\tilde{\mathbf{B}}\mathbf{Q}_j^T + \mathbf{A}_M\mathbf{D}^{-(L-1)}\tilde{\mathbf{R}}_s\mathbf{Q}_j^T \tag{21}$$

where $r_{s,k} \stackrel{\text{def}}{=} E\{s_k(t)s_k^*(t)\}$, $\bar{\rho}_{\ell,j} \stackrel{\text{def}}{=} \bar{\boldsymbol{\beta}}^H\mathbf{a}_{\ell,j}^*$, with $\bar{\boldsymbol{\beta}} \stackrel{\text{def}}{=} [\beta_1,\ldots,\beta_{K_1},0,\ldots,0]^T$, $\tilde{\mathbf{B}} \stackrel{\text{def}}{=} \text{diag}\,[\beta_1,\ldots,\beta_{K_1},0,\ldots,0]$, and $\tilde{\mathbf{R}}_s \stackrel{\text{def}}{=} \text{diag}\,[0,\ldots,0,r_{s_{K_1+1}},\ldots,r_{s_K}]$. Therefore, the rank of $\mathbf{R}_{f,j}$ still equals K. Similarly, the matrices $\tilde{\mathbf{R}}_{f,j}$, $\mathbf{R}_{b,j}$ and $\tilde{\mathbf{R}}_{b,j}$ are also of rank K.

3.2. Estimating direction cosines

The matrix $\mathbf{R}$ defined in (20) can be expressed compactly as $\mathbf{R} = \mathbf{A}_M\boldsymbol{\Gamma}$, where

$$\boldsymbol{\Gamma} = [\boldsymbol{\Gamma}_{f,1},\ldots,\boldsymbol{\Gamma}_{f,3},\tilde{\boldsymbol{\Gamma}}_{f,1},\ldots,\tilde{\boldsymbol{\Gamma}}_{f,3},\boldsymbol{\Gamma}_{b,1},\ldots,\boldsymbol{\Gamma}_{b,3},\tilde{\boldsymbol{\Gamma}}_{b,1},\ldots,\tilde{\boldsymbol{\Gamma}}_{b,3}] \tag{22}$$

with

$$\begin{aligned}\boldsymbol{\Gamma}_{f,j} &= \rho_{L,j} r_s \mathbf{B}\mathbf{Q}_j^T \\ \tilde{\boldsymbol{\Gamma}}_{f,j} &= \rho_{1,j} r_s \mathbf{B}\mathbf{D}\mathbf{Q}_j^T \\ \boldsymbol{\Gamma}_{b,j} &= \rho_{1,j}^* r_s \mathbf{B}^*\mathbf{D}^{-(L-1)}\mathbf{Q}_j^T \\ \tilde{\boldsymbol{\Gamma}}_{b,j} &= \rho_{L,j}^* r_s \mathbf{B}^*\mathbf{D}^{-(L-2)}\mathbf{Q}_j^T \end{aligned} \tag{23}$$

To exploit the propagator method for direction finding, we need dividing the $3(M-1)\times K$ array manifold $\mathbf{A}_M$ into three $(M-1)\times K$ sub-array manifolds such that each sub-array manifold corresponds to a single component of measurement (pressure or one of the components of particle velocity) at a vector hydrophone. For this purpose, we define

$$\bar{\mathbf{A}}_M = \mathbf{E}^T \mathbf{A}_M \tag{24}$$

where $\mathbf{E}$ is an exchange matrix defined as

$$\begin{aligned}\mathbf{E} = [&\mathbf{e}_1, \mathbf{e}_4, \ldots, \mathbf{e}_{3(M-1)-2}, \mathbf{e}_2, \mathbf{e}_5, \ldots, \mathbf{e}_{3(M-1)-1}, \\ &\mathbf{e}_3, \mathbf{e}_6, \ldots, \mathbf{e}_{3(M-1)}]\end{aligned} \tag{25}$$

and $\mathbf{e}_n$ is the $3(M-1)$ dimensional unit vector whose nth element is 1 and other elements are zero. The matrix $\bar{\mathbf{A}}_M$, which is a row-exchanged version of $\mathbf{A}_M$ may be partitioned as

$$\bar{\mathbf{A}}_M = [\bar{\mathbf{A}}_{M,1}^T, \bar{\mathbf{A}}_{M,2}^T, \bar{\mathbf{A}}_{M,3}^T]^T \tag{26}$$

where

$$\bar{\mathbf{A}}_{M,j} = [\mathbf{d}_j^T, \mathbf{d}_{j+3}^T, \ldots, \mathbf{d}_{j+3(M-2)}^T]^T, \quad j = 1,2,3 \tag{27}$$

and $\mathbf{d}_j$ is the jth row of $\mathbf{A}_M$. The blocks $\bar{\mathbf{A}}_{M,1}$, $\bar{\mathbf{A}}_{M,2}$, $\bar{\mathbf{A}}_{M,3}$ are related as

$$\bar{\mathbf{A}}_{M,2} = \bar{\mathbf{A}}_{M,1}\boldsymbol{\Phi}^u \tag{28}$$

$$\bar{\mathbf{A}}_{M,3} = \bar{\mathbf{A}}_{M,1}\boldsymbol{\Phi}^v \tag{29}$$

where $\boldsymbol{\Phi}^u$ and $\boldsymbol{\Phi}^v$ are, respectively, defined as

$$\boldsymbol{\Phi}^u \stackrel{\text{def}}{=} \text{diag}\,[u(\theta_1,\phi_1), \ldots, u(\theta_K,\phi_K)] \tag{30}$$

$$\boldsymbol{\Phi}^v \stackrel{\text{def}}{=} \text{diag}\,[v(\theta_1,\phi_1), \ldots, v(\theta_K,\phi_K)] \tag{31}$$

The proposed method is based on the partition of the block $\bar{\mathbf{A}}_{M,1}$ as

$$\bar{\mathbf{A}}_{M,1} = \begin{bmatrix} \bar{\mathbf{A}}_{M,1}^{(1)} \\ \bar{\mathbf{A}}_{M,1}^{(2)} \end{bmatrix} \tag{32}$$

where $\bar{\mathbf{A}}_{M,1}^{(1)}$ consists of the first K rows of $\bar{\mathbf{A}}_{M,1}$, and $\bar{\mathbf{A}}_{M,2}^{(2)}$ consists of the remaining $M-1-K$ rows. The blocks $\bar{\mathbf{A}}_{M,2}$ and $\bar{\mathbf{A}}_{M,3}$ may be partitioned in a similar manner. The matrix $\bar{\mathbf{A}}_M$ can therefore be partitioned as

$$\bar{\mathbf{A}}_M = \begin{bmatrix} \bar{\mathbf{A}}_{M,1}^{(1)} \\ \mathbf{G} \end{bmatrix} \tag{33}$$

with

$$\mathbf{G} = [(\bar{\mathbf{A}}_{M,1}^{(2)})^T, (\bar{\mathbf{A}}_{M,2}^{(1)})^T, (\bar{\mathbf{A}}_{M,2}^{(2)})^T, (\bar{\mathbf{A}}_{M,3}^{(1)})^T, (\bar{\mathbf{A}}_{M,3}^{(2)})^T]^T \tag{34}$$

where $\bar{\mathbf{A}}_{M,j}^{(1)}$ and $\bar{\mathbf{A}}_{M,j}^{(2)}$ are, respectively, the first K rows and the remaining $M-1-K$ rows of $\bar{\mathbf{A}}_{M,j}$ $(j=1,2,3)$.

It is easy to find that $\bar{\mathbf{A}}_{M,1}^{(1)}$ is a $K\times K$ Vandermonde matrix and hence it is a full rank matrix. Therefore, the first K rows of $\bar{\mathbf{A}}_M$ are linearly independent and the other rows of $\bar{\mathbf{A}}_M$ can be expressed as linear combinations of the first K rows. The $(3(M-1)-K)\times K$ propagator matrix $\mathbf{P}$ can be defined as a unique linear operator which relates the matrices $\bar{\mathbf{A}}_{M,1}^{(1)}$ and $\mathbf{G}$ through the Eq. [16]

$$\mathbf{P}^H \bar{\mathbf{A}}_{M,1}^{(1)} = \mathbf{G} \tag{35}$$

Using (28), (29) and (33), (34), we have

$$\mathbf{G} = [(\bar{\mathbf{A}}_{M,1}^{(2)})^T, (\bar{\mathbf{A}}_{M,1}^{(1)}\boldsymbol{\Phi}^u)^T, (\bar{\mathbf{A}}_{M,1}^{(2)}\boldsymbol{\Phi}^u)^T, (\bar{\mathbf{A}}_{M,1}^{(1)}\boldsymbol{\Phi}^v)^T, (\bar{\mathbf{A}}_{M,1}^{(2)}\boldsymbol{\Phi}^v)^T]^T \tag{36}$$

On the other hand, we can partition the Hermitian transpose of the propagator $\mathbf{P}$, i.e., $\mathbf{P}^H$, as

$$\mathbf{P}^H = [\mathbf{P}_1^T, \mathbf{P}_2^T, \mathbf{P}_3^T, \mathbf{P}_4^T, \mathbf{P}_5^T]^T \tag{37}$$

where $\mathbf{P}_1$–$\mathbf{P}_5$ have the dimensions identical to $\bar{\mathbf{A}}_{M,1}^{(2)}$, $\bar{\mathbf{A}}_{M,1}^{(1)}\boldsymbol{\Phi}^u$, $\bar{\mathbf{A}}_{M,1}^{(2)}\boldsymbol{\Phi}^u$, $\bar{\mathbf{A}}_{M,1}^{(1)}\boldsymbol{\Phi}^v$ and $\bar{\mathbf{A}}_{M,1}^{(2)}\boldsymbol{\Phi}^v$, respectively.

Eqs. (35), (36) and (37) together yield

$$\mathbf{P}_1\bar{\mathbf{A}}_{M,1}^{(1)} = \bar{\mathbf{A}}_{M,1}^{(2)} \tag{38}$$

$$\mathbf{P}_2\bar{\mathbf{A}}_{M,1}^{(1)} = \bar{\mathbf{A}}_{M,1}^{(1)}\boldsymbol{\Phi}^u \tag{39}$$

$$\mathbf{P}_3\bar{\mathbf{A}}_{M,1}^{(1)} = \bar{\mathbf{A}}_{M,1}^{(2)}\boldsymbol{\Phi}^u \tag{40}$$

$$\mathbf{P}_4\bar{\mathbf{A}}_{M,1}^{(1)} = \bar{\mathbf{A}}_{M,1}^{(1)}\boldsymbol{\Phi}^v \tag{41}$$

$$\mathbf{P}_5\bar{\mathbf{A}}_{M,1}^{(1)} = \bar{\mathbf{A}}_{M,1}^{(2)}\boldsymbol{\Phi}^v \tag{42}$$

Using the pair (38) and (40), we can obtain[3]

$$\mathbf{P}_1^\dagger\mathbf{P}_3 = \mathbf{A}_{M,1}^{(1)}\boldsymbol{\Phi}^u(\mathbf{A}_{M,1}^{(1)})^{-1} \tag{43}$$

Similarly, using the pair (38) and (42), we have

$$\mathbf{P}_1^\dagger\mathbf{P}_5 = \mathbf{A}_{M,1}^{(1)}\boldsymbol{\Phi}^v(\mathbf{A}_{M,1}^{(1)})^{-1} \tag{44}$$

Eqs. (43) and (44) suggest that the direction cosines along the x-axis and the y-axis, which constitute the diagonal elements of $\boldsymbol{\Phi}^u$ and $\boldsymbol{\Phi}^v$, are equal to the eigenvalues of matrices $\mathbf{P}_1^\dagger\mathbf{P}_3$ and $\mathbf{P}_1^\dagger\mathbf{P}_5$. Eqs. (43) and (44) also establish the relationships between the propagator and the direction cosines.

In order to estimate the propagator, we define a new matrix

$$\bar{\mathbf{R}} = \mathbf{E}^T\mathbf{R} \tag{45}$$

[3] From Eqs. (39) and (41), we have

$$\mathbf{P}_2 = \bar{\mathbf{A}}_{M,1}^{(1)}\boldsymbol{\Phi}^u(\bar{\mathbf{A}}_{M,1}^{(1)})^{-1}$$

$$\mathbf{P}_4 = \bar{\mathbf{A}}_{M,1}^{(1)}\boldsymbol{\Phi}^v(\bar{\mathbf{A}}_{M,1}^{(1)})^{-1}$$

These two equations imply that the direction cosines along the x-axis and the y-axis are also equal to the eigenvalues of matrices $\mathbf{P}_2$ and $\mathbf{P}_4$. Therefore, the direction cosines can also be estimated from $\mathbf{P}_2$ and $\mathbf{P}_4$.

where $\mathbf{E}$ is defined in (25). Hence

$$\bar{\mathbf{R}} = \mathbf{E}^T\mathbf{R} = \mathbf{E}^T\mathbf{A}_M\mathbf{\Gamma} = \mathbf{A}_M\mathbf{\Gamma} = \begin{bmatrix} \bar{\mathbf{A}}_{M,1}^{(1)} \\ \mathbf{P}^H\bar{\mathbf{A}}_{M,1}^{(1)} \end{bmatrix}\mathbf{\Gamma} \tag{46}$$

Similarly, we partition $\bar{\mathbf{R}}$ into

$$\bar{\mathbf{R}} = \begin{bmatrix} \bar{\mathbf{R}}_1 \\ \bar{\mathbf{R}}_2 \end{bmatrix} \tag{47}$$

where $\bar{\mathbf{R}}_1$ and $\bar{\mathbf{R}}_2$ are, respectively, the first K and the last $3(M-1)-K$ rows of $\bar{\mathbf{R}}$.

From (35) and (47), we have

$$\bar{\mathbf{R}}_2 = \mathbf{P}^H\bar{\mathbf{R}}_1 \tag{48}$$

Thus, the propagator can be found from $\bar{\mathbf{R}}_1$ and $\bar{\mathbf{R}}_2$ as

$$\mathbf{P} = (\bar{\mathbf{R}}_1\bar{\mathbf{R}}_1^H)^{-1}\bar{\mathbf{R}}_1\bar{\mathbf{R}}_2^H \tag{49}$$

With the estimation of the propagator $\hat{\mathbf{P}}$ from the sample data, the x-axis direction cosines $\{u_k, k=1,\ldots,K\}$ can be found from the K eigenvalues of $\hat{\mathbf{P}}_1^{\dagger}\hat{\mathbf{P}}_3$, and the y-axis direction cosines $\{v_k, k=1,\ldots,K\}$ can be found from the K eigenvalues of $\hat{\mathbf{P}}_1^{\dagger}\hat{\mathbf{P}}_5$.[4]

3.3. Azimuth–elevation angles estimation

It is seen from (43) and (44) that the matrices $\mathbf{P}_1^{\dagger}\mathbf{P}_3$ and $\mathbf{P}_1^{\dagger}\mathbf{P}_5$ have the same set of eigenvectors. Eigenvalues of these matrices corresponding to the same eigenvector therefore give the direction cosines of the same signal. However, the matrices $\hat{\mathbf{P}}_1^{\dagger}\hat{\mathbf{P}}_3$ and $\hat{\mathbf{P}}_1^{\dagger}\hat{\mathbf{P}}_5$, which are obtained from the finite-data, would have different sets of eigenvectors. Let $\mathbf{T}^u$ and $\mathbf{T}^v$ denote the matrices whose columns are formed by the eigenvectors of $\hat{\mathbf{P}}_1^{\dagger}\hat{\mathbf{P}}_3$ and $\hat{\mathbf{P}}_1^{\dagger}\hat{\mathbf{P}}_5$, respectively. Equations corresponding to (43) and (44) can be written as [4,5]

$$\hat{\mathbf{P}}_1^{\dagger}\hat{\mathbf{P}}_3 = \mathbf{T}^u\mathbf{\Phi}^u(\mathbf{T}^u)^{-1} \tag{50}$$

$$\hat{\mathbf{P}}_1^{\dagger}\hat{\mathbf{P}}_5 = \mathbf{T}^v\mathbf{\Phi}^v(\mathbf{T}^v)^{-1} \tag{51}$$

The matching set of eigenvectors corresponding to each signal can be obtained by matching the columns of $\mathbf{T}^u$ and $\mathbf{T}^v$. Consider the matrix products $(\mathbf{T}^u)^{-1}\mathbf{T}^v$, and let i_k denote the column indices of the matrix elements with the largest absolute values in the kth rows of $(\mathbf{T}^u)^{-1}\mathbf{T}^v$. It is inferred that the eigenvectors constituting the kth column of $\mathbf{T}^u$ and the i_kth column of $\mathbf{T}^v$, correspond to the same signal. Hence, for each $k \in \{1,2,\ldots,K\}$, the eigenvalues corresponding to the kth column of $\mathbf{T}^u$ and the i_kth column of $\mathbf{T}^v$ are the estimates $\{\hat{u}_k, \hat{v}_k\}$ of the direction cosines of the kth signal.

From the foregoing analysis, the kth signal's 2D directions can be estimated as [4,5]

$$\hat{\theta}_k = \arcsin(\sqrt{\hat{u}_k^2 + \hat{v}_k^2}) \tag{52}$$

and

$$\hat{\phi}_k = \angle(\hat{u}_k + j\hat{v}_k) \tag{53}$$

Note that the azimuth estimates and the elevation estimates are automatically matched without any additional processing.

3.4. Implementation of the proposed algorithm

Assuming that the number of signals is known or correctly estimated, the proposed algorithm with the finite array data can be summarized as follows.

(1) Estimate the vectors $\mathbf{r}_{fm,j}$, $\tilde{\mathbf{r}}_{fm,j}$, $\mathbf{r}_{bm,j}$ and $\tilde{\mathbf{r}}_{bm,j}$ as

$$\begin{aligned}
\hat{\mathbf{r}}_{fm,j} &= \frac{1}{N}\sum_{n=1}^{N}\mathbf{z}_{fm}(t_n)z_{L,j}^*(t_n), \quad m=1,\ldots,M-1,\ j=1,2,3\\
\hat{\tilde{\mathbf{r}}}_{fm,j} &= \frac{1}{N}\sum_{n=1}^{N}\mathbf{z}_{fm}(t_n)z_{1,j}^*(t_n), \quad m=2,\ldots,M,\ j=1,2,3\\
\hat{\mathbf{r}}_{bm,j} &= \frac{1}{N}\sum_{n=1}^{N}z_{1,j}(t_n)\mathbf{z}_{bm}(t_n), \quad m=1,\ldots,M-1,\ j=1,2,3\\
\hat{\tilde{\mathbf{r}}}_{bm,j} &= \frac{1}{N}\sum_{n=1}^{N}z_{L,j}(t_n)\mathbf{z}_{bm}(t_n), \quad m=2,\ldots,M,\ j=1,2,3
\end{aligned} \tag{54}$$

(2) For each m and j, form the matrices

$$\begin{aligned}
\hat{\mathbf{R}}_{fm,j} &= [\mathbf{J}_1\hat{\mathbf{r}}_{fm,j}, \mathbf{J}_2\hat{\mathbf{r}}_{fm,j}, \ldots, \mathbf{J}_K\hat{\mathbf{r}}_{fm,j}]\\
\hat{\tilde{\mathbf{R}}}_{fm,j} &= [\mathbf{J}_1\hat{\tilde{\mathbf{r}}}_{fm,j}, \mathbf{J}_2\hat{\tilde{\mathbf{r}}}_{fm,j}, \ldots, \mathbf{J}_K\hat{\tilde{\mathbf{r}}}_{fm,j}]\\
\hat{\mathbf{R}}_{bm,j} &= [\mathbf{J}_1\hat{\mathbf{r}}_{bm,j}, \mathbf{J}_2\hat{\mathbf{r}}_{bm,j}, \ldots, \mathbf{J}_K\hat{\mathbf{r}}_{bm,j}]\\
\hat{\tilde{\mathbf{R}}}_{bm,j} &= [\mathbf{J}_1\hat{\tilde{\mathbf{r}}}_{bm,j}, \mathbf{J}_2\hat{\tilde{\mathbf{r}}}_{bm,j}, \ldots, \mathbf{J}_K\hat{\tilde{\mathbf{r}}}_{bm,j}]
\end{aligned} \tag{55}$$

(3) For each j, construct $\hat{\mathbf{R}}_{f,j}$, $\hat{\tilde{\mathbf{R}}}_{f,j}$, $\hat{\mathbf{R}}_{b,j}$ and $\hat{\tilde{\mathbf{R}}}_{b,j}$ using (13), (17), (18) and (19), respectively, and then form $\hat{\mathbf{R}}$ using (20).

(4) Calculate the row-exchanged version of $\hat{\mathbf{R}}$ as $\hat{\tilde{\mathbf{R}}} = \mathbf{E}^T\hat{\mathbf{R}}$. Estimate the propagator $\mathbf{P}$ as $\hat{\mathbf{P}} = (\hat{\bar{\mathbf{R}}}_1\hat{\bar{\mathbf{R}}}_1^H)^{-1}\hat{\bar{\mathbf{R}}}_1\hat{\bar{\mathbf{R}}}_2^H$, where $\hat{\bar{\mathbf{R}}}_1$ and $\hat{\bar{\mathbf{R}}}_2$ are, respectively, the first K and the last $3(M-1)-K$ rows of $\hat{\bar{\mathbf{R}}}$.

(5) Partition $\hat{\mathbf{P}}$ to obtain the estimates, $\hat{\mathbf{P}}_1$, $\hat{\mathbf{P}}_2$, $\hat{\mathbf{P}}_3$, $\hat{\mathbf{P}}_4$ and $\hat{\mathbf{P}}_5$. Estimate the x-axis direction cosines can be from the K eigenvalues of $\hat{\mathbf{P}}_1^{\dagger}\hat{\mathbf{P}}_3^H$ or $\hat{\mathbf{P}}_2$ and estimate the y-axis direction cosines from the K eigenvalues of $\hat{\mathbf{P}}_1^{\dagger}\hat{\mathbf{P}}_5^H$ or $\hat{\mathbf{P}}_4$.

(6) Pair the x-axis direction cosines with the y-axis direction cosines, and compute the kth signal's azimuth and elevation angles using (52) and (53).

3.5. Computational complexity analysis

Most vector hydrophone direction finding algorithms require to compute the correlations of all array data, the resulting needed correlations are therefore $(3L)^2$. However, in the proposed algorithm, only the cross-correlations between some array data are needed. In detail, evaluating the matrix $\mathbf{R}_{f,j}$ and $\tilde{\mathbf{R}}_{b,j}$, $j=1,2,3$ requires the

[4] Alternatively, we can estimate the x-axis and y-axis direction cosines from the eigenvalues of matrices $\hat{\mathbf{P}}_2$ and $\hat{\mathbf{P}}_4$, respectively.

correlations between the data of the first to the $(L-1)$th hydrophone and those of the Lth hydrophone; evaluating the matrix $\tilde{\mathbf{R}}_{f,j}$ and $\mathbf{R}_{b,j}, j=1,2,3$ requires the correlations between the data of the second to the Lth hydrophone and those of the first hydrophone. The total number of needed correlations is $36L-54$, which is smaller than $(3L)^2$.

Another advantage of the proposed algorithm is that it does not require any eigen-decomposition of the cross covariance matrix to extract the signal or noise subspaces. The number of multiplications involved in calculating the propagator $\mathbf{P}$ is in the order of $3(M-1)KN$, i.e., $3(M-1)KN$ [16]. In contrast, the subspace-based algorithms, like MUSIC and ESPRIT, the major computation required by the eigen-decomposition of covariance matrix results in $O(3(M-1)^2N)$ multiplications. It follows under typical condition $M \gg K$ that the ratio of the computational requirement of the proposed algorithm to the subspace-based algorithm is $O(K/3(M-1))$. This result is interesting for the case that the number of hydrophone sensors is large and/or the number of signals is small.

4. Simulations

Performance of the proposed propagator algorithm is evaluated by comparing to the particle-velocity-field smoothing (PVFS) [14] based propagator algorithm and SUMWE algorithm [19]. For the proposed algorithm, a ULA with 16 vector hydrophones, separated by $\Delta=\sqrt{\Delta_x^2+\Delta_y^2}$ is used. For the PVFS-propagator method, an L-shape array geometry, with 16 vector hydrophones uniformly placed vector hydrophones along x-axis for estimating u_k and 16 vector hydrophones uniformly placed along y-axis for estimating v_k is considered. For SUMWE algorithm, an L-shape array geometry, with 24 pressure hydrophones uniformly placed vector hydrophones along x-axis for estimating u_k and 24 pressure hydrophones uniformly placed along y-axis for estimating v_k is used. Hence, the hardware costs of the SUMWE algorithm and the presented algorithm are comparable. The inter-element displacement for PVFS-propagator and SUMWE algorithms is a half-wavelength, since these two algorithms would suffer angle ambiguities when the spacing is larger than 0.5λ. Two equal-power narrowband coherent signals impinge with parameters $\theta_1=52.67^\circ$, $\phi_1=39.90^\circ$, $\theta_2=65.21^\circ$, $\phi_2=40.53^\circ$, i.e., with direction cosines $u_1=0.61$, $v_1=0.51$, $u_2=0.69$, $v_2=0.59$. The emitted signals are narrowband, temporally white, full-correlated, zero-mean, complex-value, Gaussian-distributed stochastic processes. Each data point in each graph is averaged over 500 independent Monte-Carlo trials. The performance metric used is the root mean squared error (RMSE) of kth signal, which is defined as

$$\mathrm{RMSE}_k=\sqrt{\frac{1}{2P}\sum_{p=1}^{P}\{(\hat{u}_k(p)-u_k)^2+(\hat{v}_k(p)-v_k)^2\}} \tag{56}$$

where $\hat{u}_k(p)$ and $\hat{v}_k(p)$ are the direction cosines of the kth source estimated from the pth Monte-Carlo trial, and P is the number of total Monte-Carlo trials.

Fig. 1 plots the RMSEs of the proposed algorithm with different inter-hydrophone spacing against SNR levels. It is seen from the figure that the estimation errors of the proposed algorithm decrease as the inter-hydrophone spacing increases. This estimation accuracy enhancement can be intuitively explained as the array aperture extension. The array aperture extension is commonly known to offer improved DOA estimation precision, but may lead to a set of cyclically ambiguous DOA estimates for conventional pressure hydrophone. However, for vector hydrophone, the proposed algorithm suffers no DOA cyclical ambiguity even the inter-hydrophone spacing exceeding the Nyquist half-wavelength upper limit. This fact is because the proposed algorithm yields the DOA estimates from the steering vectors of the vector hydrophones.

Figs. 2 and 3, respectively, plot the RMSEs of the proposed algorithm, the PVFS-propagator algorithm and the SUMWE algorithm versus SNR and snapshot number. In addition, plotted in these two figures include CRB, which is computed using the array geometry for the proposed algorithm. For the proposed algorithm, we set the inter-hydrophone spacing of the proposed algorithm

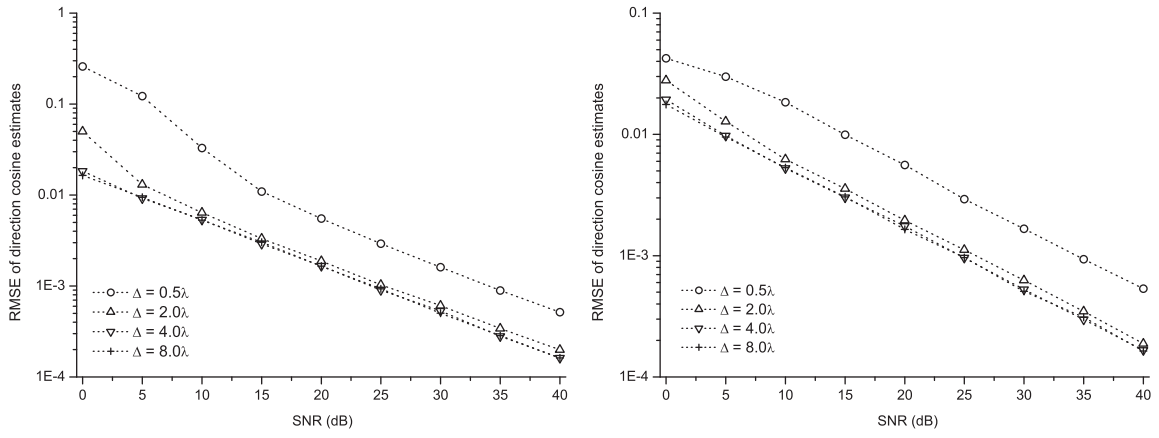

Fig. 1. RMSEs of direction cosine estimates versus SNRs. Two signals with parameters $\theta_1=52.67^\circ$, $\phi_1=39.90^\circ$, $\theta_2=65.21^\circ$, $\phi_2=40.53^\circ$, signal 1 (left), signal 2 (right).

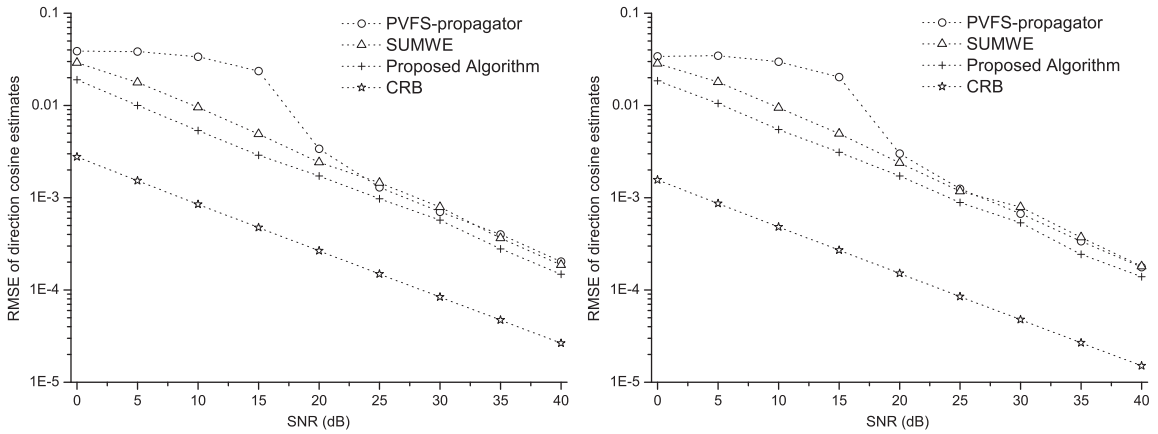

Fig. 2. RMSEs of the proposed algorithm, PVFS-propagator algorithm and SUMWE algorithm against SNRs. Two signals with parameters $\theta_1 = 52.67^\circ$, $\phi_1 = 39.90^\circ$, $\theta_2 = 65.21^\circ$, $\phi_2 = 40.53^\circ$, signal 1 (left), signal 2 (right).

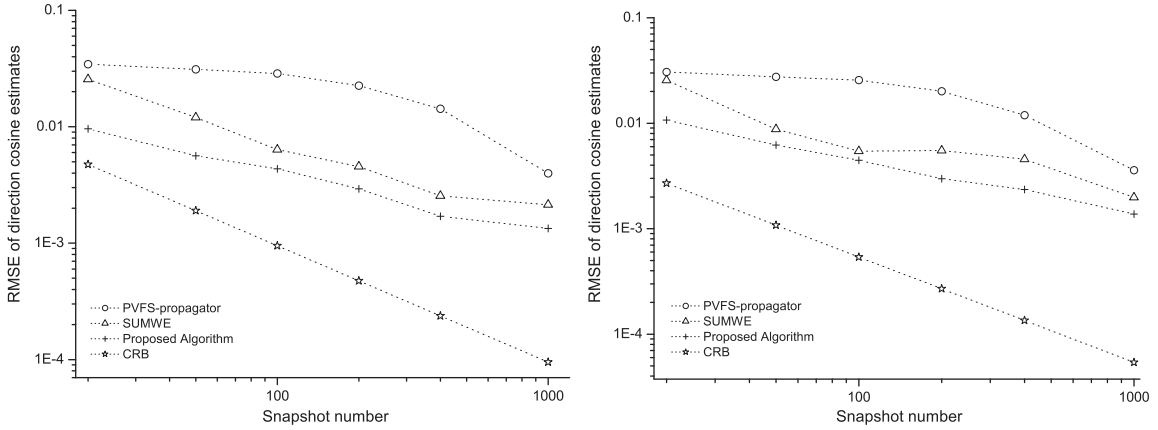

Fig. 3. RMSEs of the proposed algorithm, PVFS-propagator algorithm and SUMWE algorithm at different snapshot numbers. Two signals with parameters $\theta_1 = 52.67^\circ$, $\phi_1 = 39.90^\circ$, $\theta_2 = 65.21^\circ$, $\phi_2 = 40.53^\circ$, signal 1 (left), signal 2 (right).

as four wavelengths. In Fig. 2, we set snapshots $N = 200$, and in Fig. 3, we set SNR $= 15$ dB. The curves in these two figures unanimously demonstrate that the proposed algorithm can offer performance superior to those of the PVFS-propagator algorithm and SUMWE algorithm, in terms of lower estimation errors. Incidently, as the estimate errors of the proposed algorithm are a bit bigger than CRB, the proposed algorithm might be biased.

5. Conclusions

The proposed direction finding algorithm uses a uniformly linear array of vector hydrophones to estimate azimuth–elevation angles of multiple coherent signals. The coherent signals are decorrelated by subarray averaging, and the direction cosines embedded in the acoustical particle-velocity components of the vector hydrophone are estimated by exploiting the propagator method. The proposed algorithm requires neither the eigen-decomposition into signal/noise subspaces nor the 2D iteratively searching, and can offer high azimuth–elevation estimation accuracy by setting vector hydrophones to space much farther apart than a half-wavelength. Incidently, the proposed algorithm can be considered as an improvement of SUMWE algorithm [19] via replacing the pressure hydrophones there by vector hydrophones.

References

[1] R.O. Schmidt, Multiple emitter location and signal parameter estimation, IEEE Trans. Antennas Propag. 34 (March 1986) 276–280.
[2] R. Roy, T. Kailath, ESPRIT—estimation of signal parameters via rotational invariance techniques, IEEE Trans. Acoust. Speech Signal Process. 37 (July 1989) 984–995.
[3] A. Nehorai, E. Paldi, Acoustic vector sensor array processing, IEEE Trans. Signal Process. 42 (9) (September 1994) 2481–2491.
[4] K.T. Wong, M.D. Zoltowski, Closed-form underwater acoustic direction-finding with arbitrarily spaced vector hydrophones at unknown locations, IEEE J. Oceanic Eng. 22 (3) (July 1997) 566–575.
[5] K.T. Wong, M.D. Zoltowski, Extended-aperture underwater acoustic multi-source azimuth/elevation direction-finding using uniformly but sparsely spaced vector hydrophones, IEEE J. Oceanic Eng. 22 (4) (October 1997) 659–672.
[6] K.T. Wong, M.D. Zoltowski, Root-MUSIC-based azimuth–elevation angle-of-arrival estimation with uniformly spaced but arbitrarily oriented velocity hydrophones, IEEE Trans. Signal Process. 47 (12) (December 1999) 3250–3260.

[7] K.T. Wong, M.D. Zoltowski, Self-initiating velocity-field beamspace music for underwater acoustic direction-finding with irregularly spaced vector hydrophones, IEEE J. Oceanic Eng. 25 (2) (April 2000) 262–273.
[8] P. Tichavsky, K.T. Wong, M.D. Zoltowski, Near-field/far-field azimuth and elevation angle estimation using a single vector hydrophone, IEEE Trans. Signal Process. 49 (11) (November 2001) 2498–2510.
[9] M.D. Zoltowski, K.T. Wong, Closed-form eigenstructure-based direction finding using arbitrary but identical subarrays on a sparse uniform rectangular array grid, IEEE Trans. Signal Process. 48 (8) (August 2000) 2205–2210.
[10] H.W. Chen, J.W. Zhao, Coherent signal-subspace processing of acoustic vector sensor array for DOA estimation of wideband sources, Signal Process. 85 (2005) 837–847.
[11] B. Champagne, Adaptive eigendecomposition of data covariance matrices based on first-order perturbations, IEEE Trans. Signal Process. 42 (10) (October 1994) 2758–2770.
[12] P. Comon, G.H. Golub, Tracking a few extreme singular values and vectors in signal processing, Proc. IEEE 78 (8) (August 1990) 1327–1343.
[13] B. Yang, Projection approximation subspace tracking, IEEE Trans. Signal Process. 43 (1) (January 1995) 95–107.
[14] J. Tao, W. Chang, Y. Shi, Direction-finding of coherent sources via 'particle-velocity-field smoothing', IET Radar Sonar Navig. 2 (2) (April 2008) 127–134.
[15] J. Munier, G.Y. Delisle, Spatial analysis using new properties of the cross-spectral matrix, IEEE Trans. Signal Process. 39 (3) (March 1991) 746–749.
[16] S. Marcos, A. Marsal, M. Benidir, The propagator method for source bearing estimation, Signal Process. 42 (1995) 121–138.
[17] P. Li, J. Sun, B. Yu, Two-dimensional spatial spectrum estimation of coherent signals without spatial smoothing and eigendecomposition, IEE Proc. Radar Sonar Navig. 143 (5) (October 1996) 295–299.
[18] Y. Wu, G. Liao, H.C. So, A fast algorithm for 2-D direction-of-arrival estimation, Signal Process. 83 (2003) 1827–1831.
[19] J.M. Xin, A. Sano, Computationally efficient subspace-based method for direction-of-arrival estimation without eigendecomposition, IEEE Trans. Signal Process. 52 (4) (2004) 876–893.
[20] N. Tayem, H.M. Kwon, L-shape two-dimensional arrival angle estimation with propagator method, IEEE Trans. Antennas Propag. 53 (5) (May 2005) 1622–1630.